New Mn- and rare-earth-rich epidote-group minerals in metacherts: manganiandrosite-(Ce) and vanadoandrosite-(Ce)

Bénédicte CENKI-TOK[1, 2], Alain RAGU[3], Thomas ARMBRUSTER[4], Christian CHOPIN[1, *] and Olaf MEDENBACH[5]

[1] Laboratoire de Géologie, UMR 8538 du CNRS, Ecole normale supérieure, 24 rue Lhomond, 75005 Paris, France
* Corresponding author, e-mail: chopin@geologie.ens.fr
[2] Now at: Centre de Géochimie de la surface – EOST, 1 rue Blessig, 67083 Strasbourg Cedex, France
[3] Laboratoire de Tectonique – UMR 7072 du CNRS, Université Pierre et Marie Curie, Case 129, 4 place Jussieu, 75252 Paris Cedex 05, France
[4] Laboratorium für chemische und mineralogische Kristallographie, Universität Bern, Freiestrasse 3, 3012 Bern, Switzerland
[5] Institut für Geologie, Mineralogie und Geophysik, Ruhr-Universität Bochum, 44780 Bochum, Germany

Abstract: Two new rare-earth-bearing members of the epidote group are described from carbonate pods in Mn-rich metacherts. According to the structure refinements, Mn occurs mainly in the divalent state in both of them and occupies both the large A1 site instead of Ca and the large octahedral M3 site instead of Al or Fe^{3+}, charge-compensating the substitution of Ca^{2+} by REE^{3+} in the largest, A2 site. The two minerals are therefore members of the androsite series.

Manganiandrosite-(Ce) has dominant Mn^{3+} in the M1 site; it occurs at the Praborna manganese mine, Saint-Marcel, Aosta valley, Italy, in a Mesozoic eclogite-facies ophiolitic unit of the western Alps. Associated minerals are rhodochrosite and Mn-pyroxenoid, with minor calderite, spessartine, hematite and pyrophanite. The structural formula is $^{A1}[Mn^{2+}_{0.60}Ca_{0.40}]_{\Sigma = 1}$ $^{A2}[(Ce_{0.46}La_{0.23}Nd_{0.12}Sm_{0.01})_{\Sigma REE \geq 0.82}Sr_{0.07}Ca_{0.02}]_{\Sigma \geq 0.91}$ $^{M1}[Mn^{3+}_{0.63}Fe^{3+}_{0.23}Ti_{0.10}Mg_{0.04}]_{\Sigma=1}$ $^{M2}Al_{1.00}$ $^{M3}[Mn^{2+}_{0.96}Mn^{3+}_{0.04}]_{\Sigma=1}$ $Si_2O_7SiO_4O(OH)$, ideally $^{A1}Mn^{2+}$ ^{A2}Ce $^{M1}Mn^{3+}$ ^{M2}Al $^{M3}Mn^{2+}$ $Si_2O_7SiO_4O(OH)$. Monoclinic, space group $P2_1/m$, a 8.901(2) Å, b 5.738(1) Å, c 10.068(2) Å, β 113.425(3)°, V 471.81 Å³, $Z = 2$. Biaxial positive, $2V = 80.6(1.5)°$, n(calc) = 1.80, strong pleochroism: α light yellow, β orange-brown, γ red-brown.

Vanadoandrosite-(Ce) has dominant V^{3+} in M1. It occurs at the Vielle Aure mining district, central Pyrénées, France, in and around quartz–rhodochrosite–sulphide veinlets cross-cutting the rhodochrosite ore in greenschist-facies Lower Carboniferous radiolarite. Other associated minerals are vuorelainenite, chalcopyrite, vanadian spessartine, and friedelite. The structural formula of the most V-rich crystal is $^{A1}(Mn^{2+}_{0.62}Ca_{0.38})_{\Sigma1.00}$ $^{A2}[(Ce_{0.39}La_{0.15}Nd_{0.10}Sm_{0.02})_{\Sigma REE=0.66}Ca_{0.21}Sr_{0.11}]_{\Sigma0.98}$ $^{M1}(V^{3+}_{0.80}Al_{0.16}Mg_{0.03}Ti_{0.01})_{\Sigma1.00}$ $^{M2}Al_{1.00}$ $^{M3}(Mn^{2+}_{0.36}V^{3+}_{0.31}Fe^{2+}_{0.23}Fe^{3+}_{0.10})_{\Sigma1.00}$ $Si_2O_7SiO_4O(OH)$, ideally $^{A1}Mn^{2+}$ ^{A2}Ce $^{M1}V^{3+}$ ^{M2}Al $^{M3}Mn^{2+}$ $Si_2O_7SiO_4O(OH)$. Monoclinic, space group $P2_1/m$, a 8.856(3) Å, b 5.729(2) Å, c 10.038(4) Å, β 113.088(5)°, V 468.5 Å³, $Z = 2$. Biaxial, n(calc) = 1.82, strong pleochroism: yellow-brown < red-brown < dark greenish brown //b. The root-name applies to any epidote-group mineral in which REE are dominant in A2, Mn^{2+} in A1, V^{3+} in M1, Al in M2, and in which Mn^{2+} is the dominant charge-compensating (*i.e.* divalent) cation in M3.

The structural study of these new androsites suggests that khristovite-(Ce) also has significant Mn^{2+} on A1 and should be reanalysed. Other epidote-group minerals from the Pyrenean deposits represent two new potential species, with the end-members $CaCe\,AlAlMn^{2+}\,Si_3O_{12}(OH)$, *i.e.* the $^{[M3]}Mn^{2+}$ analogue of allanite and dissakisite, and $Mn^{2+}Ce\,MgAlMn^{2+}\,Si_3O_{11}F(OH)$, *i.e.* the $^{[A1]}Mn$ analogue of khristovite. Even in these Mn-rich systems, incorporation of F on O4 is balanced by Mg and not Mn incorporation. The variety of mineral assemblages in Mn–V–REE-rich systems is discussed on the basis of oxidation state.

Key-words: epidote group, rare-earth elements, manganiandrosite-(Ce), vanadoandrosite-(Ce), new mineral, crystal structure, khristovite-(Ce).

Introduction

The incorporation of trivalent rare-earth elements (REE) in the structure of epidote-group minerals, with the general formula A1A2 M1M2M3 $SiO_4Si_2O_7(O,F)OH$, is achieved by replacement of Ca^{2+} in the large A2 site, which is charge-balanced by substitution of divalent Me^{2+} cations for Al^{3+} or Fe^{3+} in the octahedral M3 site. With Ca dominant in A1, and Al^{3+} dominant in M1 and in M2, these substitutions lead to allanite proper for Me = Fe and to dissakisite for Me = Mg

(Grew *et al.*, 1991). The case of Me = Mn, *i.e.* divalent Mn in M3, is interesting. Analyses of Mn-rich 'allanite', mostly from pegmatites and granite (*e.g.* Deer *et al.*, 1997; Hoshino *et al.*, 2006), suggest that Mn^{2+} is primarily entering the A1 site in place of Ca, whereas Fe^{2+} is still the dominant charge-balancing cation in M3. Only in 'allanites' from extremely Mn-rich rock-compositions like metamorphosed manganese ore deposits does Mn^{2+} dominate the M3 site – in addition to the A1 site – provided the oxidation state also permits Mn^{3+} (in M1). This leads to the very Mn-rich end-member $Mn^{2+}REE^{3+} Mn^{3+}AlMn^{2+} SiO_4Si_2O_7O(OH)$, which was described as androsite-(La) by Bonazzi *et al.* (1996, with La as the dominant REE). According to the nomenclature scheme most recently adopted for the epidote-group by the IMA CNMMN (Armbruster *et al.*, 2006), this mineral is renamed manganiandrosite-(La). [In the following the use of root-names without the Levinson modifier implies that the series is referred to, rather than a species].

During the study of manganese-bearing siliceous sediments metamorphosed under a variety of pressure-temperature (P-T) conditions, in the Western Alps and the Pyrénées, we found new examples of Mn-rich REE-bearing epidote-group minerals extending the range of known compositions and leading to the definition of two new species, manganiandrosite-(Ce) and vanadoandrosite-(Ce), respectively. Both minerals were approved by the IMA CNMMN (votes no. 2002-49 and 2004-15), originally under the names 'androsite-(Ce)' and 'vanadio-androsite-(Ce)'. Their present names conform with the new IMA nomenclature scheme of the epidote group (Armbruster *et al.*, 2006). Type material is deposited at the Musée de Minéralogie, Ecole des Mines de Paris, under reference numbers 73951 ENSMP and 73952 ENSMP, respectively. This paper reports the paragenesis, description and crystal structure of these new epidote-group minerals and envisages their stability in terms of oxygen fugacity.

Geological setting

Alps

The Mesozoic sedimentary sequence associated to the ophiolites of the Western Alps and northern Apennines hosts a number of manganese concentrations in radiolarites or siliceous strata. These sediments belong to the lower part of the section deposited on the Jurassic, Tethyan ocean floor, either on pillow-lavas or hydrothermally altered metabasites, or directly on gabbro or serpentinite. This sequence was metamorphosed during Eocene subduction and collision, under greenschist-facies conditions in the Apennines (*e.g.* the classical Val Graveglia district, Cortesogno *et al.*, 1979; Marchesini & Pagano, 2001) and, in the Western Alps, from lowest-grade blueschist-facies conditions in the external units (*e.g.* Martin & Polino, 1984) to eclogite-facies conditions in the internal units (Gruppo Ofioliti, 1977; Dal Piaz *et al.*, 1979), locally reaching coesite-eclogite conditions (Reinecke, 1991). The locality studied, the Praborna mine near Saint-Marcel, Val d'Aosta, Italy, belongs to the eclogite-facies ophiolitic Zermatt-Saas Unit which structurally over-

lies the Monte Rosa and Gran Paradiso internal crystalline massifs (*e.g.* Dal Piaz *et al.*, 2001). It is part of a group of small Mn ore-deposits occurring on the western tip of the Gran Paradiso massif at the upper end of the Maurienne Valley, France (Chopin, 1978), and on the north-eastern flank of the Gran Paradiso massif, on either side of the Val d'Aosta (Martin & Kiénast, 1987). The presence of eclogitic metabasite (with paragonite and glaucophane stable) and of the talc–chloritoid–garnet (± phengite) assemblage in metapelite (Chopin, 1981a, b) [the latter magnificently developed near Praborna, at the Servette mine (Martin & Tartarotti, 1989)] points to peak metamorphic conditions on the order of 15 kbar, 500°C (P > 10–12 kbar, 500–600°C; Martin & Tartarotti, 1989).

Pyrénées

The Paleozoic stratiform Mn ore deposits in the Central Pyrénées are long known for their Mn-silicates assemblages including rhodonite, tephroite, friedelite and spessartine (Lacroix, 1900). A reinvestigation (Ragu, 1990) revealed the presence of numerous additional, sometimes rare silicate species, such as helvite, hyalophane, humite-group Mn minerals, tinzenite, welinite, and of vanadium-rich phases such as the spinel vuorelainenite, an 'allanite' of unique composition to be described below, and an unknown oxide compound of Mn, Ba and V, later defined as nabiasite (Brugger *et al.*, 1999).

Numerous manganese deposits have been mined in the Lower Carboniferous jasper series of the Axial Zone of the Central Pyrénées. The workings form an E-W trending strip about 3 to 4 km wide and 15 km long straddling the Aure and Louron valleys, Hautes Pyrénées, about 100 km SW of Toulouse. The series underwent syntectonic regional low-grade low-pressure greenschist-facies metamorphism. It was later intruded by several Late Variscan granite bodies like the Bordères, Néouvielle and Tramesaygues massifs which crop out less than 5 km to the northeast, northwest and south, respectively, possibly also as undetected cupolas at shallow depth. In the area of interest, the manganese-bearing strata lie 2 to 3 km away from the contact metamorphic aureoles. Quartz, muscovite, chlorite, rare biotite and albite are the main phases in the enclosing schists.

Occurrence, parageneses and appearance

Alps: manganiandrosite-(Ce)

The Mn deposits of the Zermatt-Saas Unit occur as quartz-rich lenses intercalated within mappable layers of quartz–phengite–almandine schist in a series of calcschist and black metashale overlying bodies of serpentinite with ophicalcite and minor metabasite. The lenses show a strong compositional layering among the main phases quartz, braunite, hematite, spessartine, piemontite and locally ardennite. These 'oxidized assemblages' imply several oxidation states of manganese and essentially trivalent iron. In some lenses, a black weathering crust signals quartz-poor to quartz-free

pods that consist of rhodochrosite and Mn-silicates (pyroxmangite, rhodonite, tephroite, friedelite, humite-group minerals), or rarely of Mn-silicates (tephroite, humites, chlorite) and spinels (galaxite, jacobsite; Chopin, 1978), *i.e.* in either case 'reduced' assemblages in which Mn is entirely divalent. These mineralogical and chemical variations across the lenses most likely reflect the compositional banding of the protolith.

The Praborna mine near Saint-Marcel is a classical locality from which roméite (Damour, 1841, Brugger *et al.*, 1997), piemontite (Kenngott, 1853) and strontiomelane (Meisser *et al.*, 1999) have been described, in addition to the spectacular colour varieties of pyroxene, phengite, titanite, *etc.* (*e.g.* Mottana *et al.*, 1979). The situation and structure of the deposit, with a layered oxidized quartzite horizon containing the braunite ore but also some reduced boudins of Mn-carbonate–silicates assemblages, are basically the same as in other Mn deposits of the Zermatt-Saas Unit, yet with a greater thickness and areal extension. The reader is referred for details to the fine geological and petrological descriptions given by Martin & Kiénast (1987) and Tumiati (2005).

The sample studied (# 84-SM56) was collected on the mine dumps in 1984 by C.C. It is a two-fist-size block in which a matrix of vein quartz contains abundant brecciated fragments of a yellow, very spessartine-rich bed and a larger, about 5 cm cockade with black weathering crust. The dark greyish-brown cockade core consists of fine-grained tephroite (partly serpentinized) and rhodochrosite, with calderite, hematite and minor pyrophanite and jacobsite. It is surrounded by a centimetre-thick pink spary reaction rim of rhodochrosite and Mn-pyroxenoid passing, through increasing modal amounts of spessartine, to a yellowish outer rim. The latter is locally separated from the vein quartz by a thin veneer of hematite flakes or passes abruptly to an aggregate of spotted yellow globules (coarse hematite and poikilitic spessartine in a groundmass of pyroxenoid and late manganocummingtonite) in sharp contact on quartz-side with a string of chocolate-colour pyroxene crystals, several millimetres in size. This coarse-grained pyroxene (*ca.* Dio_{52} Joh_{15} Kan_6 Aeg_{23} Jad_4) as well as euhedral orange spessartine crystals in the vein quartz most likely crystallized in the vein, whereas the cockade represents a fragment of a reduced carbonate-rich, Si-undersaturated protolith and its successive reaction zones with the vein quartz. An allanite-looking mineral occurs both in the dark core zone of the cockade close to the pink rim (section 84-56-5), as elongated grains a few tens of μm in length associated to tephroite, Mn-pyroxenoid, hematite and calderite, and in the rhodochrosite–pyroxenoid rim (section 84-56-2) as isolated anhedral grains, one hundred μm in size, along with scattered crystals of spessartine, calderite, hematite and pyrophanite. This epidote-group mineral turned out to be manganiandrosite-(Ce). The coexistence in this and related samples of two manganoan garnets, aluminous (spessartine) and ferric (calderite, apparently new to this locality), is dealt with in a separate paper (Cenki-Tok & Chopin, 2006).

Pyrénées: vanadoandrosite-(Ce)

The Mn-bearing horizon, now lens-shaped owing to intense isoclinal folding and boudinage, consists of four superimposed parageneses (Ragu, 1990): 1) the original rhodochrosite and quartz lenses (with ghost radiolaria) in the banded radiolarian chert; 2) Mn-silicates (rhodonite, spessartine, tephroite, friedelite, braunite) that most likely developed from rhodochrosite and quartz in these lenses; 3) up to 2-cm-wide veinlets cutting the former foliation and stratification of the lenses; they are essentially made of one or more of the four minerals rhodochrosite, friedelite, quartz and rhodonite, with a variety of minor phases (alabandite, barite, chalcopyrite, chlorite, galena, helvite, hübnerite, hyalophane, Mn humite-group minerals, the Mn-V-rich 'allanite' described below as vanadoandrosite-(Ce), spessartine, sphalerite, stilpnomelane, tinzenite, vanadian mica, vuorelaineniite, welinite, plus several Ni, Co and Cu sulphosalts); 4) manganese oxides and oxyhydroxides are produced by meteoric alteration of the ore bodies.

Whereas stage 1 represents the protolith, stage-2 assemblages developed during Variscan regional metamorphism, because their preferred orientation comforms to the regional foliation and/or stratification. Stage 3 is most likely related to late hydrothermal circulations around the granitic cupolas, as suggested by the presence of Be- and W-bearing phases (helvite, hübnerite, welinite) exclusively in these vein assemblages (Ragu, 1994).

Vanadoandrosite-(Ce) occurs specifically in the Aure valley at the mine above the Vielle Aure village, in millimetre-thick quartz–rhodochrosite–sulphide veinlets cross-cutting the massive microcrystalline rhodochrosite ore [sample # VAI(E)]. It also occurs within the ore, close to the veinlets, in a few millimetre-sized quartz grains rimmed by chalcopyrite; in such instance the vanadoandrosite prisms and radial aggregates are surrounded by a myriad of micrometre-sized vuorelainenite grains, a texture suggesting a pseudomorph (sample # VAI586, Fig. 1). The mineral forms blackish, isolated stout prismatic grains, typically a few tens of μm in length, or radiating aggregates of the same size. Associated minerals are quartz, vuorelainenite, rhodochrosite, chalcopyrite, vanadian spessartine, friedelite. Vanadian and manganoan 'allanite' grains also occur in other places of the mining district but are not sufficiently V- and Mn-rich to reach the status of vanadoandrosite. They are actually much more common so that finding crystals of appropriate size, crystallinity and composition for the defmition of a vanadoandrosite end-member turned out to be a very long quest, even with the advent of CCD detectors in crystallography.

Physical properties

Given the small grain size and material paucity, a full characterization was impossible but, after electron-microprobe analysis, presumed single crystals of both epidote minerals were drilled out of petrographic thin sections (Medenbach, 1986) for optical and X-ray diffraction study.

Manganiandrosite-(Ce) is dark brown with reddish brown streak and vitreous to adamantine lustre. It is brittle,
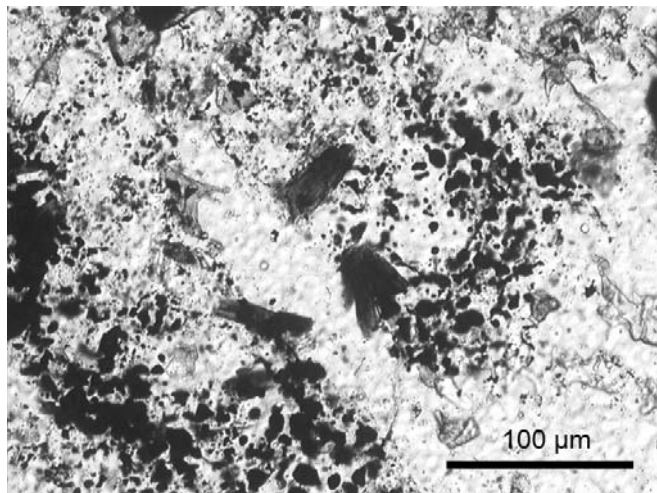
Fig. 1. Mineral assemblage in a quartz grain in the rhodochrosite ore (photomicrograph, sample VAI586, Vielle Aure, Pyrénées). Vanado-androsite-(Ce) occurs as dark translucent prisms (centre of the picture), the minute opaque grains forming a crescent around it are vuo-relainenite. The high-relief blebs in quartz in the lower right part of the picture are rhodochrosite.

no cleavage was observed; the calculated density is 4.21 g/cm³ using the analysis, 4.31 g/cm³ assuming that the non-analysed rare earths are the elements required to obtain complete occupancy of the A2 site, as compatible with the structure refinement. The mineral is transparent, non-fluorescent under the electron beam. It could not be optically completely characterized because of the strong absorption and high refractive index. It is biaxial positive, $\alpha > 1.74$; n_{calc} (Mandarino, 1976) = 1.80. The pleochroism is strong with α light yellow, β orange-brown, γ red-brown; 2V (meas.) = 80.6(1.5)° for a wavelength of 589 nm. Conoscopic figures on several grains of androsite-(Ce) in thin section were all ambiguous, but spindle-stage work on the holotype crystal shows that the light yellow colour is in the obtuse bisectrix, red-brown in the acute bisectrix. Combined with the fact that in all observed sections n(yellow) < n(brown), the obtuse bisectrix is α, therefore the positive sign for mangani-androsite-(Ce) – unlike manganiandrosite-(La), negative according to Bonazzi *et al.* (1996). Given the high 2V angle and the chemical variability, it is clear that the optical sign cannot be diagnostic.

Vanadoandrosite-(Ce). Two V-dominant crystals could be extracted from samples VAI(E) and VAI586 but, as only the former gave a decent diffraction pattern, VAI(E) was made the holotype sample even if, admittedly, VAI586 is by far closer to the vanadium end-member (see below). Vana-doandrosite is very dark brown to black, with brown streak and vitreous to adamantine lustre. It is brittle, no cleavage was observed; the calculated density is 4.27 g/cm³ for the holotype composition. The mineral is transparent in thin section, non-fluorescent under the electron beam. It is biaxial, $\alpha > 1.74$ (589 nm); the mean calculated refractive index is 1.82 for the holotype composition. Pleochroism is strong, yellow-brown < red-brown < dark greenish brown // *b*. The high refringence and strong absorption have not allowed further optical characterization.
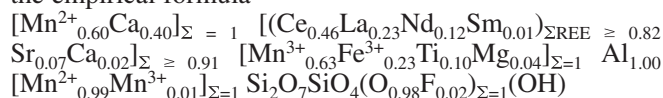
In practice, chemical analysis and/or crystal-structure refinement are necessary for species identification. Vanado-androsite and androsite are optically similar to allanite but the paragenesis is characteristic: in metamorphosed oxidized Al-poor Mn-ores, any allanite-looking mineral may well be a member of the androsite subgroup. Highly oxidising conditions [with, *e.g.*, hematite, braunite, calderitic garnet, medaite (V^{5+})] will favour manganiandrosite *sensu stricto*, less oxidising ones vanadoandrosite. The greenish hue in the pleochroic scheme of vanadoandrosite may be a hint for distinction from manganiandrosite.
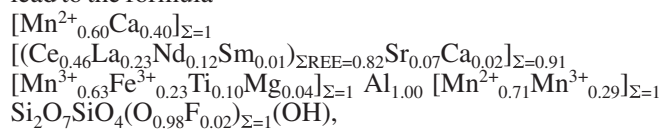
Mineral chemistry

Electron-microprobe analyses were carried out in wave-length-dispersive mode with the Cameca SX50 instrument at Centre Camparis, Paris, at 15 kV, 10 nA beam current for vanadoandrosite, 35 nA for androsite, using the following standards: diopside (Mg, Si and Ca $K\alpha$), anorthite or ortho-clase (Al $K\alpha$), vanadinite (V $K\alpha$), MnTiO₃ (Ti and Mn $K\alpha$), hematite (Fe $K\alpha$), SrSiO₃ (Sr $L\alpha$), monazite (Ce $L\alpha$ or $L\beta$), La₃ReO₈ (La $L\alpha$), NdCu (Nd $L\beta$), Sm₃ReO₈ (Sm $L\beta$), topaz or CaF₂ (F $K\alpha$). The analytical totals are somewhat low for all REE-rich epidote-group minerals; the A2 cations are possibly underestimated (by omission of minor REE, Pb, U, Th) as only the main REE and Sr were analysed among the heavy elements. Vanadium is considered trivalent on the basis of the parageneses and crystallography; iron and then manganese are partitioned between di- and trivalent states for charge balance of structural formulae calculated on an Si₃O₁₁(O,F)OH basis. This partitioning is made in Table 1 on the basis of the elements actually analysed; in the text, for comparison and unless otherwise specified, the valence par-titioning used in the formulae is based on the assumption of complete occupancy of the A2 site (by the minor non-ana-lysed rare-earths), which is signalled by the use of ΣREE≥ instead of ΣREE= in the formulae. Material paucity pre-vented direct determination of H₂O, which is calculated from stoichiometry.

Manganiandrosite-(Ce). Analysis 1 in Table 1 is the aver-age of four point analyses of the holotype crystal, drilled from section 84-56-2. Calcium is remarkably low and man-ganese, regardless of valence state, is very dominant among the potential octahedral M cations (Mg, Al, Ti, V, Mn, Fe), the sum of which clearly exceeds the stoichiometric value of 3 pfu. The excess, 0.60 pfu of the larger-size cation Mn^{2+}, is therefore assigned to the A1 site, which is then filled with Ca. The remaining Ca is assigned to the larger-size A2 site, along with Sr and REE, giving a total of 0.91 pfu in A2. Site assignment of the octahedral cations is then straightforward, if one uses the increasing size of the M2, M1 and M3 sites in the epidote group as a guide. Aluminium exactly fills M2; Fe^{3+}, Ti and Mg can then be assigned to M1, which is filled with Mn, made trivalent. The remaining Mn fills M3, with a divalent/trivalent ratio that should grossly reflect the pro-portion of trivalent to divalent cations in A2. The exact cal-culation of this ratio must take into account the presence of minor non-trivalent cations in M1 (Ti and Mg), the possible replacement of the O4 atom by F, and it may be biased by the

incomplete filling of A2, as the latter is most likely an artefact due to non-analysed minor REE (for comparison manganiandrosite-(La) bears 1.3 wt% Pr_2O_3, Bonazzi *et al.*, 1996). Assuming for the calculation of this Mn^{2+}/Mn^{3+} ratio full occupancy in A2, *i.e.* 0.91 REE pfu (marginally consistent with the structure refinement, see below), we propose the empirical formula
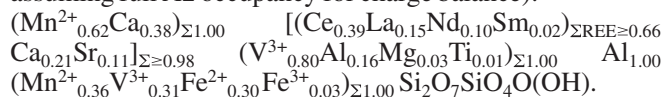
$[Mn^{2+}_{0.60}Ca_{0.40}]_{\Sigma = 1}$ $[(Ce_{0.46}La_{0.23}Nd_{0.12}Sm_{0.01})_{\Sigma REE \geq 0.82}Sr_{0.07}Ca_{0.02}]_{\Sigma \geq 0.91}$ $[Mn^{3+}_{0.63}Fe^{3+}_{0.23}Ti_{0.10}Mg_{0.04}]_{\Sigma=1}$ $Al_{1.00}$ $[Mn^{2+}_{0.99}Mn^{3+}_{0.01}]_{\Sigma=1}$ $Si_2O_7SiO_4(O_{0.98}F_{0.02})_{\Sigma=1}(OH)$

which leads to the end-member formula: $Mn^{2+}Ce$ $Mn^{3+}AlMn^{2+}$ $Si_2O_7SiO_4O(OH)$. The key features of this REE-epidote, namely dominant Mn^{2+} in A1 and M3, and dominant Mn^{3+} in M1, are robust, whatever the recalculation scheme. Indeed, the largest source of uncertainty on the Me^{2+}/Me^{3+} ratio in M3 is the assumption on the absence or presence of vacancies at the A2 site. Assuming vacancies, *i.e.* that no element would be missing in the analysis, would lead to the formula

$[Mn^{2+}_{0.60}Ca_{0.40}]_{\Sigma=1}$ $[(Ce_{0.46}La_{0.23}Nd_{0.12}Sm_{0.01})_{\Sigma REE=0.82}Sr_{0.07}Ca_{0.02}]_{\Sigma=0.91}$ $[Mn^{3+}_{0.63}Fe^{3+}_{0.23}Ti_{0.10}Mg_{0.04}]_{\Sigma=1}$ $Al_{1.00}$ $[Mn^{2+}_{0.71}Mn^{3+}_{0.29}]_{\Sigma=1}$ $Si_2O_7SiO_4(O_{0.98}F_{0.02})_{\Sigma=1}(OH)$,

in which the key cations at the various sites are the same as above. These dominant site populations are confirmed by the structure analysis (see below) and point therefore to the Ce analogue of manganiandrosite-(La), *i.e.* manganiandrosite-(Ce) according to Levinson's rule.

Vanadoandrosite-(Ce). The single point analysis of the tiny holotype crystal is reported in Table 1 (anal. 2) together with the range of 8 analyses obtained from the 6 crystals in the same thin section (VAI-E), and one point analysis (no. 4) standing for three similar analyses of the most V-rich crystals in sample VAI586. The impressive V_2O_3 contents (> 14 wt%) in the latter imply more than 1 V pfu and raise the question of vanadium partitioning among the octahedral sites. Recasting the analysis along the same scheme as for manganiandrosite leads again to dominant (0.63 pfu) Mn^{2+} in A1; M2 is filled by Al, the excess Al together with Mg and Ti is assigned to M1, which is filled with 0.80 V^{3+}; the excess V^{3+} (0.31 pfu) is in turn assigned to M3, which is then filled with Fe (0.34) and the remainder of Mn (0.36). To charge balance the REE in A2, the whole Mn in M3 must be made divalent and most of the Fe as well, which supports Fe and Mn assignment to M3 in the present case, as summarized by the structural formula (recalculated on a 3 Si basis, assuming full A2 occupancy for charge balance):

$(Mn^{2+}_{0.62}Ca_{0.38})_{\Sigma1.00}$ $[(Ce_{0.39}La_{0.15}Nd_{0.10}Sm_{0.02})_{\Sigma REE=0.66}Ca_{0.21}Sr_{0.11}]_{\Sigma \geq 0.98}$ $(V^{3+}_{0.80}Al_{0.16}Mg_{0.03}Ti_{0.01})_{\Sigma1.00}$ $Al_{1.00}$ $(Mn^{2+}_{0.36}V^{3+}_{0.31}Fe^{2+}_{0.30}Fe^{3+}_{0.03})_{\Sigma1.00}Si_2O_7SiO_4O(OH)$.

We end up with V^{3+} overwhelmingly dominant in M1 but with a very compounded population in M3, in which Mn^{2+} is the dominant charge-compensating cation. As long as one assumes that the largest charge-compensating M cations (Fe^{2+} and Mn^{2+}) must occupy the largest M site (M3), the above site allocation is quite robust, because Mg is so low that it does not matter whether it is assigned to M1 or M3. Interestingly, whether some Fe is assigned to M3 or to M1 (in place of V moving to M3) could apparently matter, as V would remain largely dominant in M1 but would become the dominant cat-

ion in M3 too. However, Mn^{2+} remains in any event the *dominant charge-compensating* cation at this site.

As structural analysis of this material proved impossible, we had to resort to the other sample to establish a partitioning scheme with support from structure refinement. The analysis of the holotype VAI(E) crystal in Table 1 has much lower V and higher Mn (and lower Ca) than VAI586. Recasting it like the previous ones (assuming complete occupancies in A sites for calculation of the Me^{3+}/Me^{2+} ratio) leads to the formula $(Mn^{2+}_{0.69}Ca_{0.29})_{\Sigma \geq 0.98}$ $(Ce_{0.62}La_{0.32}Nd_{0.03})_{\Sigma \geq 0.97}$ $(V^{3+}_{0.44}Mg_{0.19}Al_{0.18}Fe^{3+}_{0.17}Mn^{3+}_{0.02})_{\Sigma1.00}$ $Al_{1.00}$ $Mn^{2+}_{1.00}$ $Si_2O_7SiO_4(O_{0.81}F_{0.19})_{\Sigma1.00}(OH)$.

The main features in it, namely dominant Mn^{2+} in A1 and in M3, dominant V^{3+} along with Mg in M1 are again quite robust, they are sensible in terms of ionic radii and, gratifyingly, are definitely confirmed by the results of site-scattering refinement (see below). The presence of Mg in M1 and in amounts comparable to the F contents does not seem to be fortuitous, as there is a correlation of Mg and F contents in the analyses of this sample (from 0.19 Mg/0.19 F to 0.30 Mg/0.27 F pfu). This is evidence for the F Mg = O Al substitution, which relates dissakisite, CaREE Al_2Mg $Si_2O_7SiO_4O(OH)$, to dollaseite, CaREE MgAlMg $Si_2O_7SiO_4F(OH)$ (Peacor & Dunn, 1988). Regardless of this minor substitution, considering that dominant Mn^{2+} in both A1 and M3 is an attribute unique to androsite, we felt that the root-name vanadoandrosite is fitting for the end-member $Mn^{2+}REE$ $V^{3+}AlMn^{2+}$ $Si_2O_7SiO_4O(OH)$ and any epidote-group mineral in which REE are dominant in A2, Mn^{2+} in A1, V^{3+} in M1, Al in M2 and in which Mn^{2+} is the dominant charge-compensating cation in M3.

Crystal structure

Structural data for both new minerals were collected with a Siemens Smart CCD single-crystal X-ray diffractometer. Experimental details are summarized in Table 2. The diffraction patterns of both crystals were of rather low quality as the spots were fairly broad and slightly streaked. It is not clear whether this is a characteristic of the minerals or whether this is caused by the heavy mechanical strain due to milling and extraction of very small fragments from the thin section. Electron microprobe analyses (Table 1) were performed on the same crystal fragment as structurally analysed. After measurement of more than a hemisphere of diffraction data, an empirical absorption correction based on a pseudo psi-scan-technique was applied. Multiple measurements of equivalent reflections were used to calculate a transmission ellipsoid for intensity correction. The structure was solved by direct methods. Diffraction data were in agreement with space group $P2_1/m$ known for all other monoclinic members of the epidote group. For the structure refinement (Sheldrick, 1997) Ce was assigned to A2, Mn to A1, M2, and M3, and Al to M2. If the refined population indicated complete occupancy, the corresponding parameter was fixed. Determined populations were transferred to site-scattering values. In particular, there are strong inverse correlations between the scale factor and the occupancy of A2. Thus, the refined standard deviation for this variable is cer-

Table 1. Analyses (wt%) and formulae of Mn- and REE-rich epidote-group minerals (and coexisting garnet).

Sample	84-SM56-2, holot. xtal Manganiandrosite-(Ce)		VAI(E) Vanadoandrosite-(Ce)		Garnet*	VAI 586	CP 851	VAI N86	Kato et al., 1994 'Vanadoallanite'		Hasegawa in Deer et al.,1997	
	Mean of 4 anal.	Range of 4 anal.	Holotype crystal	Range on 6 crystals		V-rich analysis	Mean of 3 anal.	Mean of 3 anal.	Core	Rim	1958	1957
Anal. no.	1		2		3	4	5	6	7	8	9	10
SiO_2	29.04	28.7–29.3	28.81	28.8–29.5	36.35	31.02	32.24	29.18	31.59	30.69	30.78	30.32
Al_2O_3	8.20	7.6–8.5	9.65	9.1–10.6	19.28	10.14	19.36	9.40	11.10	9.75	15.44	15.89
V_2O_3			5.30	3.1–5.3	1.37	14.36	1.19	2.26	9.58	8.83		
TiO_2	1.26	0.8–1.5	0.06	0.03–0.07	0.02	0.17	0.20	0.04			0.26	0.04
Fe_2O_3 *	2.98	1.9–3.4	2.18	1.6–3.2	0.58	1.44	2.42	0.36	3.85	7.56	3.48	3.77
FeO*						2.82	0.25		6.74	4.57	10.95	10.81
MnO*	15.01	14.0–15.8	17.78	17.3–23.2	42.26	11.92	11.58	21.04	5.43	6.48	6.52	6.06
Mn_2O_3*	11.62	11.4–12.9	1.75					1.87				
MgO	0.28	0.2–0.4	1.22	1.2–2.9	0.07	0.19	0.33	4.22	0.31	0	0.07	0.32
SrO	1.17	0.4–1.7	0	0–0.07		1.99	0.43	0.04				
CaO	3.82	3.6–4.2	2.57	2.4–4.6	0.87	5.69	9.35	0.75	9.77	8.56	4.90	4.28
Ce_2O_3	12.22	11.8–13.0	16.14	14.0–16.1		11.08	8.83	17.26	14.30	13.67	8.72	7.44
La_2O_3	6.08	5.6–6.4	8.29	7.4–8.8		4.12	6.47	2.35	6.27	5.33	11.63	14.74
Nd_2O_3	3.24	3.0–3.7	0.84	0.7–1.1		2.78	2.34	4.48	0.87	2.17		
Sm_2O_3	0.18	0–0.4	0	0–0.1		0.56	0.34					
Y_2O_3						0	0.14				2.98	1.85
ThO_2											2.04	1.70
F	0.07	0–0.14	0.57	0.6–1.5	0.17		0.29	2.01				
H_2O*	[1.45]		[1.44]			[1.55]	[1.61]	[1.46]	[1.58]	[1.53]	1.54	1.89
Sum – F=O	96.59	95.8–98.0	96.36	94.3–97.3	100.90	99.83	97.25	95.89	101.39	99.14	99.57	99.35
Si	3.000		3.000		2.983	3.000	3.000	3.000	3.000	3.000	3.000	3.000
Al	0.998		1.184		1.866	1.156	2.123	1.138	1.242	1.123	1.774	1.853
V			0.442		0.090	1.113	0.089	0.186	0.729	0.692		
Ti	0.098		0.005		0.002	0.012	0.014	0.003			0.019	0.003
Fe^{3+}	0.232		0.171		0.036	0.105	0.169	0.028	0.275	0.556	0.255	0.281
Fe^{2+}						0.228	0.019		0.535	0.374	0.893	0.894
Mn^{2+}	1.313		1.568		2.938	0.976	0.913	1.832	0.437	0.537	0.538	0.508
Mn^{3+}	0.914		0.138					0.146				
Mg	0.043		0.189		0.009	0.027	0.046	0.647	0.044	0.000	0.010	0.047
Sr	0.070		0.000			0.112	0.023	0.002				
Ca	0.423		0.287		0.077	0.590	0.932	0.083	0.994	0.897	0.512	0.454
Ce	0.462		0.615			0.392	0.301	0.650	0.497	0.489	0.311	0.270
La	0.232		0.318			0.147	0.222	0.089	0.220	0.192	0.418	0.538
Nd	0.120		0.031			0.096	0.078	0.164	0.030	0.076		
Sm	0.006		0.000			0.019	0.011					
Y						0.000	0.007				0.155	0.097
Th											0.045	0.038
F	0.023		0.188		0.044		0.084	0.653			H =1.171	1.407
Σ cat.	7.911		7.950		8.000	7.974	7.946	7.970	8.003	7.936	7.930	7.983

* Fe and Mn oxidation ratios, [H_2O] contents and formulae calculated on a $Si_3O_{11}(O,F)OH$ + electroneutrality basis, excepted Hasegawa on a 3 Si basis and garnet on an 8-cation basis.

Table 2. Parameters for X-ray data collection and crystal-structure refinement.

Mineral	Manganiandrosite-(Ce)	Vanadoandrosite-(Ce)
Diffractometer	Siemens Smart CCD	Siemens Smart CCD
X-ray radiation	Mo$K\alpha$ (0.71073 Å)	Mo$K\alpha$ (0.17073 Å)
X-ray power	50 kV, 40 mA	50 kV, 40 mA
Temperature	293 K	293 K
Crystal size	$20 \times 60 \times 100$ μm	$20 \times 50 \times 80$ μm
Detector to sample distance	5.44 cm	5.44 cm
Rotation axis	omega	omega
Rotation width	0.3°	0.3°
Total number of frames	1271	1271
Frame size	512×512 pixels	512×512 pixels
Time per frame	60 s	360 s
Space group	$P2_1/m$	$P2_1/m$
Cell dimensions		
a (Å)	8.901(2)	8.856(3)
b (Å)	5.738(1)	5.729(2)
c (Å)	10.068(2)	10.038(4)
β (°)	113.425(3)	113.088(4)
Volume Å^3	471.81	468.5
Collection mode	hemisphere	hemisphere
Reflections collected	2656	3188
Max. 2 θ	55.88	55.93
Index range	$-10 \leq h \leq 11$	$-11 \leq h \leq 11$
	$-7 \leq k \leq 6$	$-6 \leq k \leq 7$
	$-13 \leq l \leq 10$	$-13 \leq l \leq 11$
Unique reflections	1147	1153
Reflections $> 4\sigma(F)$	664	1000
R_{int} %	7.7	8.0
$R\sigma$ %	16.1	7.4
Number of least squares parameters	85	85
GooF	0.77	1.25
$R1$ %, I $> 4\sigma(I)$	3.86	6.67
$R1$ %, all data	8.53	8.18
w$R2$ % (on F^2)	6.48	15.6
A (weight parameter)[1]	0.009	0.0663
B (weight parameter)[1]	0	3.76
$+\Delta$ e$^-$ (residual density)	1.5 close to A2 (Ce)	3 close to A2 (Ce)
$-\Delta$ e$^-$ (residual density)	-1 close to O8	-1.5 close to A2 (Ce)

[1] Weight = $1 / (\sigma^2(F_o^2) + (A \times P)^2 + B \times P)$; P = (Max $(F_o^2, 0)$ + $2 \times F_c^2)/3$

Table 3a. Atomic coordinates and B_{eq} for manganiandrosite-(Ce).

Atom	x	y	z	B_{eq} (Å^2)
A1	0.7594(3)	3/4	0.1531(3)	1.14(6)
A2	0.5920(1)	3/4	0.4282(1)	1.05(2)
Si1	0.3490(5)	3/4	0.0325(4)	0.73(8)
Si2	0.6932(5)	1/4	0.2828(5)	0.84(8)
Si3	0.1929(5)	3/4	0.3248(4)	0.57(9)
M1	0	0	0	1.03(5)
M2	0	0	1/2	0.8(1)
M3	0.3167(3)	1/4	0.2066(3)	1.06(5)
O1	0.2456(8)	0.989(1)	0.0212(7)	1.0(1)*
O2	0.3162(7)	0.972(1)	0.3596(6)	0.7(1)*
O3	0.8060(8)	0.012(1)	0.3322(7)	1.0(1)*
O4	0.057(1)	1/4	0.132(1)	1.1(2)*
O5	0.050(1)	3/4	0.1588(9)	1.0(2)*
O6	0.079(1)	3/4	0.421(1)	0.4(2)*
O7	0.516(1)	3/4	0.176(1)	1.1(2)*
O8	0.559(1)	1/4	0.347(1)	1.2(2)*
O9	0.400(1)	3/4	-0.106(1)	1.2(2)*
O10	0.091(1)	1/4	0.428(1)	0.5(2)*

Note: * Starred atoms were refined isotropically. Number of electrons refined on various metal sites: A1: 23(1); A2: 52(1); M1: 25(1); M2: 13; M3: 25(1)

Table 3b. Atomic coordinates and B_{eq} for vanadoandrosite-(Ce).

Atom	x	y	z	B_{eq} (Å^2)
A1	0.7634(4)	3/4	0.1541(3)	1.39(7)
A2	0.5926(1)	3/4	0.4286(1)	1.11(2)
Si1	0.3467(6)	3/4	0.0319(5)	0.95(7)
Si2	0.6951(5)	1/4	0.2842(5)	0.85(7)
Si3	0.1907(5)	3/4	0.3216(5)	0.99(7)
M1	0	0	0	1.15(9)
M2	0	0	1/2	0.87(7)
M3	0.3179(3)	1/4	0.2050(3)	1.22(7)
O1	0.243(1)	0.990(1)	0.0211(9)	1.3(1)*
O2	0.314(1)	0.972(1)	0.3574(9)	1.4(1)*
O3	0.8056(9)	0.011(1)	0.3315(9)	1.1(1)*
O4	0.058(1)	1/4	0.137(1)	1.3(1)*
O5	0.050(1)	3/4	0.157(1)	1.1(1)*
O6	0.081(1)	3/4	0.421(1)	1.2(1)*
O7	0.515(1)	3/4	0.173(1)	1.3(1)*
O8	0.560(1)	1/4	0.354(1)	1.4(1)*
O9	0.398(1)	3/4	-0.107(1)	1.4(1)*
O10	0.092(1)	1/4	0.433(1)	1.1(1)*

Note: * Starred atoms were refined isotropically. Number of electrons refined on various metal sites: A1: 23(1); A2: 58; M1: 18(1); M2: 13; M3: 25(1)

tainly underestimated. Because of limited data quality and to maintain a reasonable ratio between observed reflections and number of least squares parameters, anisotropic displacement parameters were only refined for metal sites. Hydrogen positions were not evaluated for the same reasons. Atomic coordinates are summarized in Table 3, anisotropic displacement parameters in Table 4, and calculated bond lengths in Table 5. Due to the small size of the available crystals powder X-ray diffraction data were calculated with the program LAZY-PULVERIX (Yvon *et al.*, 1977) from the refined crystal structures and are summarized in Table 6.

Manganiandrosite-(Ce)

The chemically determined composition implies *ca*. 51 electrons on A2, which would on the first glance nicely match the refined site scattering on A2 of 52(1) electrons. However, as mentioned above, the latter value should be regarded with caution due to correlation problems. Thus, the data quality is not sufficient to decide whether the A2 site is completely occupied (missing heavy elements in the electron-microprobe analyses) or whether it is partly vacant as suggested by the chemical data taken at face value. Site scat-

Table 4a. Anisotropic displacement parameters for manganiandrosite-(Ce).

Atom	U_{11}	U_{22}	U_{33}	U_{12}	U_{13}	U_{23}
A1	0.022(2)	0.009(2)	0.014(2)	0	0.009(1)	0
A2	0.0149(7)	0.0123(6)	0.0110(6)	0	0.0034(5)	0
Si1	0.012(3)	0.006(3)	0.010(2)	0	0.004(2)	0
Si2	0.014(3)	0.006(2)	0.012(2)	0	0.006(2)	0
Si3	0.014(3)	0.003(2)	0.008(2)	0	0.006(2)	0
M1	0.017(1)	0.006(1)	0.016(1)	0.000(1)	0.007(1)	0.000(1)
M2	0.015(3)	0.003(2)	0.013(3)	-0.001(2)	0.005(2)	0.000(2)
M3	0.016(1)	0.008(1)	0.013(1)	0	0.002(1)	0

Table 4b. Anisotropic displacement parameters for vanadoandrosite-(Ce).

Atom	U_{11}	U_{22}	U_{33}	U_{12}	U_{13}	U_{23}
A1	0.021(2)	0.012(1)	0.012(2)	0	0.007(1)	0
A2	0.0114(5)	0.0135(5)	0.0135(5)	0	0.0008(4)	0
Si1	0.010(2)	0.009(2)	0.012(2)	0	-0.002(2)	0
Si2	0.009(2)	0.009(2)	0.012(2)	0	0.000(2)	0
Si3	0.011(2)	0.013(2)	0.012(2)	0	0.003(2)	0
M1	0.011(2)	0.013(2)	0.016(2)	-0.001(1)	0.016(1)	-0.002(1)
M2	0.008(2)	0.008(2)	0.012(2)	-0.003(2)	-0.002(2)	-0.001(2)
M3	0.014(1)	0.012(1)	0.014(2)	-0.001(2)	0.002(1)	0

tering values (Table 3) for all other cation sites are in excellent agreement with the measured chemical composition.

Vanadoandrosite-(Ce)

According to the structure refinement A2 is fully occupied by REE, M3 by Mn, and M2 by Al, which confirms electron-microprobe analyses. The site scattering on M1 of 18(1) electrons is also in good agreement with the assumed composition $V^{3+}_{0.44}Mg_{0.19}Al_{0.18}Fe_{0.17}Mn_{0.02}$ for this site, yielding 19.5 electrons.

Structural comparison

Although there are only cell dimensions for three androsite minerals available, manganiandrosite-(La) (Bonazzi et al., 1996), manganiandrosite-(Ce), and vanadoandrosite-(Ce), all three minerals have a monoclinic β angle < 114° in common. Most other epidote-group minerals have β > 114.5° (excluding solid solution with androsite). There is one exception, another Mn-rich mineral with β = 113.4° (Sokolova et al., 1991) which will be discussed below.

The bonding angle Si-O-Si in the disilicate group was derived from model calculations on $H_6Si_2O_7$ to exhibit a flat energetic valley between ca. 125° and 170° (Gibbs, 1982). The largest angle of this type (Si1-O9-Si2) in epidote-group minerals is found for clinozoisite with 161.9(1)° (e.g. Comodi & Zanazzi, 1997) and the smallest one (137°) for manganiandrosite-(Ce) and vanadoandrosite-(Ce). Considering the different types of homo- and heterovalent substitutions in epidote-group minerals, there is a fairly striking correlation between the Si1-O9-Si2 angle and the mean bond length of the M3 octahedron (Fig. 2). The mechanism causing the variation in the Si-O-Si angle is a rotation of the rods of edge-sharing octahedra around the **b** axis (Bonazzi et al., 1996). Small Si1-O9-Si2 angles lead to a more anisotropically deformed cavity, which is occupied by the A1 cation. The deformed A1 cavity allows smaller cations (e.g., Mn^{2+})
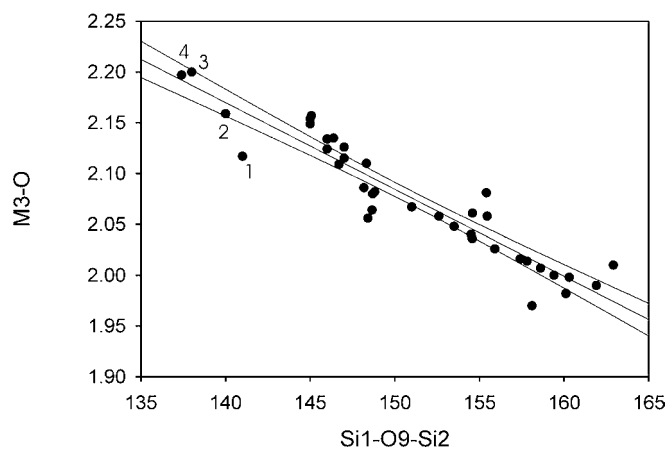

Fig. 2. Dependence of the average M3-O (Å) distance from the bending angle Si1-O9-Si2 (°) in epidote-group minerals; central line (linear regression) adjacent lines border 95 % probability. Structural data were retrieved from the literature. Clinozoisite and epidote data (29 structures) were taken from Gabe et al. (1973), Carbonin & Molin (1980), Stergiou et al. (1987), Bonazzi & Menchetti (1995), and Comodi & Zanazzi (1997). Allanite data (7 structures) are from Bonazzi & Menchetti (1995), piemontite and strontiopiemontite data (12 structures) are from Catti et al. (1988, 1989), Ferraris et al. (1989), Bonazzi et al. (1990, 1992). In addition, Pb- and REE-rich piemontite (Bermanec et al., 1994), dollaseite-(Ce) (Peacor & Dunn, 1988), REE-rich piemontite and androsite-(La) (#2) (Bonazzi et al., 1996), khristovite-(Ce) (#3) (Sokolova et al., 1991), dissakisite-(Ce) (Rouse & Peacor, 1993), ferriallanite-(Ce) (#1) (Kartashov et al., 2002), manganiandrosite-(Ce) (#4), and vanadoandrosite-(Ce) (#4) (this study) were selected.

Table 5. Selected bond distances (Å) and angles.

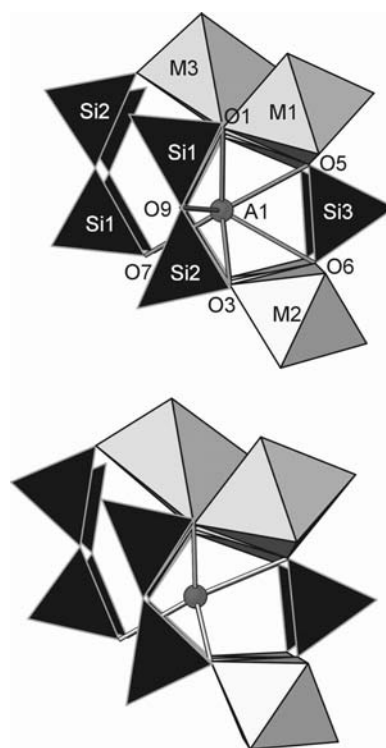| Mineral	Manganiandrosite-(Ce)	Vanadoandrosite-(Ce)
A1–O3 2×	2.256(7)	2.242(8)
A1–O7	2.267(9)	2.285(11)
A1–O1 2×	2.294(6)	2.287(8)
A1–O5	2.561(6)	2.518(11)
Mean (six bonds)	2.322	2.310
A1–O6	3.048(8)	3.035(8)
A1–O9 2×	3.152(8)	3.154(8)
A1–O9'	3.224(8)	3.266(8)
Mean (ten bonds)	2.652	2.647
A2–O7	2.354(9)	2.377(12)
A2–O2 2×	2.527(6)	2.539(8)
A2–O2' 2×	2.604(6)	2.614(8)
A2–O10	2.607(9)	2.587(11)
A2–O3 2×	2.878(6)	2.862(8)
A2–O8 2×	2.965(2)	2.946(3)
mean	2.691	2.689
Si1–O7	1.609(10)	1.605(13)
Si1–O9	1.629(10)	1.627(12)
Si1–O1 2×	1.630(7)	1.639(8)
mean	1.625	1.628
Si2–O8	1.572(9)	1.608(12)
Si2–O9	1.638(10)	1.643(13)
Si2–O3 2×	1.651(7)	1.640(8)
mean	1.628	1.633
Si3–O2 2×	1.627(6)	1.619(8)
Si3–O5	1.651(9)	1.639(12)
Si3–O6	1.656(9)	1.648(11)
mean	1.640	1.631
M1–O4 2×	1.885(6)	1.914(8)
M1–O5 2×	2.061(6)	2.045(8)
M1–O1 2×	2.112(6)	2.075(8)
mean	2.019	2.011
M2–O3 2×	1.877(6)	1.883(8)
M2–O6 2×	1.905(6)	1.905(7)
M2–O10 2×	1.925(6)	1.894(7)
mean	1.902	1.894
M3–O8	2.056(10)	2.078(13)
M3–O4	2.131(9)	2.133(11)
M3–O2 2×	2.218(6)	2.221(8)
M3–O1 2×	2.278(7)	2.257(8)
mean	2.197	2.195
Si1–O9–Si2	137.4(6)°	137.4(8)°

Fig. 3. Deformation of the A1 cavity depending on the Si1-O9-Si2 angle. Upper figure: clinozoisite with nine-fold coordination of A1. Lower figure: manganiandrosite-(Ce) with six-fold coordination of A1. Both structures projected along **b**.

to nestle close to the cavity wall, leading to distorted sixfold coordination. In contrast, for large Si1-O9-Si2 angles the coordination of A1 is more properly interpreted as nine-fold (Fig. 3).

Bonazzi *et al.* (1996) and Bonazzi & Menchetti (2004) use the length difference between the seventh (A1-O6) and the sixth longest (A1-O5) distance as parameter (δ_{7-6}) to estimate the amount of Mn^{2+} on A1. Their regression line indi-cates $\delta_{7-6} = 0.32$ for piemontite (without Mn^{2+}) and extrapolates to 0.60 for complete occupancy by Mn^{2+}. Corresponding δ_{7-6} values for manganiandrosite-(Ce) and vanadoandrosite-(Ce) are 0.487 and 0.517, respectively. In other words, δ_{7-6} values above 0.46 are characteristic of androsite with > 0.5 Mn^{2+} on A1. The higher δ_{7-6} values for vanadoandrosite-(Ce) also agrees with the composition of A1 (0.69 Mn^{2+} + 0.29 Ca) compared to (0.60 Mn^{2+} + 0.40 Ca) for manganiandrosite-(Ce).

The crystal structure of a new epidote-group mineral with $\beta = 113.4°$ (Sokolova *et al.*, 1991), later named khristovite-(Ce) (Pautov *et al.*, 1993), also exhibits a very narrow Si1-O9-Si2 angle of 137°. This observation is consistent with the occupancy of M3 by Mn^{2+}. In addition, the coordination of A1 may be described as six-fold with an average distance of 2.33 Å. This value is very similar to the corresponding one of 2.32 Å for manganiandrosite-(La) (Bonazzi *et al.*, 1996) or manganiandrosite-(Ce) (this study) and 2.31 Å for vanadoandrosite-(Ce). For comparison, ferriallanite-(Ce) (Kartashov *et al.*, 2002) has A1 almost completely occupied by Ca yielding an average A1-O distance of the six-shortest bonds of 2.40 Å. The δ_{7-6} value of the mineral by Sokolova *et al.* (1991) is 0.51. The diagram to estimate Mn^{2+} on A1 given by Bonazzi *et al.* (1996) clearly suggests > 0.5 Mn^{2+} on A1 for the new mineral described by Sokolova *et al.* (1991). Unfortunately, the chemical composition given by the latter authors appears rather non-stoichiometric and it is also not clear whether structural study and chemical analysis were performed on the very same fragment. They assumed 0.6 Ca + 0.2 La + 0.2 vacancies on A1. The X-ray scattering power

Table 6. Calculated X-ray powder pattern for manganiandrosite-(Ce) and vanadoandrosite-(Ce), $CuK\alpha_1$ radiation, Debye-Scherrer geometry, only intensities $I/I_o > 5$. The ten strongest reflections are marked in bold.

h	k	l	d (Å) Mangani-androsite-(Ce)	I/Io	d (Å) Vanado-androsite-(Ce)	I/Io	h	k	l	d (Å) Mangani-androsite-(Ce)	I/Io	d (Å) Vanado-androsite-(Ce)	I/Io
0	0	1	9.2382	8	9.2340	**25**	4	0	-1	2.1852	23	2.1765	21
1	0	0	8.1674	11	8.1467	**24**	1	2	-3	2.1805	7	2.1759	5
1	0	-1	7.8639	**28**	7.8159	19	2	2	1	2.1604	20	2.1581	17
1	0	1	5.1815	**23**	5.1833	19	0	1	4	2.1425	6	2.1412	6
1	0	-2	4.9517	12	4.9310	7	4	0	-3	2.1376	6	2.1247	5
0	1	1	4.8743	7	4.8682	8	2	2	-3	2.1144	16	2.1075	19
1	1	0	4.6951	16	4.6863	17	0	2	3	2.0991	16	2.0969	14
0	0	2	4.6191	14	4.6170	10	2	0	3	2.0913	8	2.0925	10
2	0	-2	3.9319	5			2	2	2	1.9228	13	1.9218	16
1	1	-2	3.7488	9	3.7373	11	1	1	4	1.9070	6	1.9073	7
0	1	2	3.5981	9	3.5949	11	3	1	2			1.9051	5
2	1	-1	3.5141	**41**	3.5004	**43**	2	2	-4	1.8744	10	1.8686	9
2	1	0	3.3271	12	3.3198	14	0	2	4	1.7991	5		
2	0	1	3.2834	8	3.2818	11	4	2	-2	1.7571	5		
2	1	-2			3.2284	5	2	3	-1	1.7569	6	1.7532	6
2	0	-3	3.1282	5			4	1	-5	1.6845	7	1.6755	6
3	0	-2	2.9042	**24**	2.8872	**21**	2	0	-6	1.6776	5	1.6728	6
1	1	-3	2.8964	**100**	2.8890	**100**	4	2	0	1.6636	5	1.6599	5
0	2	0	2.8690	**35**	2.8645	**41**	1	3	-3	1.6616	13	1.6585	13
2	1	1	2.8498	13	2.8477	14	5	1	-1	1.6571	5	1.6512	5
0	2	1	2.7399	6	2.7359	5	3	2	2	1.6518	10	1.6508	8
3	0	0	2.7225	14	2.7156	10	1	0	-6	1.6361	10	1.6336	9
0	1	3	2.7134	**39**	2.7114	**31**	0	3	3	1.6248	5	1.6227	5
1	2	0	2.7069	**39**	2.7023	**34**	4	2	-4	1.6217	23	1.6142	21
3	1	-1	2.6225	**53**	2.6124	**54**	3	3	-1	1.6046	12	1.6007	12
3	0	-3			2.6053	6	1	1	5	1.5993	8	1.5995	9
2	0	2	2.5908	**28**	2.5916	**26**	4	1	2	1.5784	8	1.5775	8
1	0	-4	2.4975	5	2.4921	5	4	0	-6			1.5559	6
1	2	-2	2.4824	8	2.4769	5	5	2	-1	1.4820	5		
0	2	2	2.4372	6			2	2	-6	1.4482	7	1.4445	7
3	1	-3	2.3843	12	2.3716	11	0	4	0	1.4345	16	1.4323	15
2	2	-2	2.3176	14	2.3103	12	2	1	5	1.4306	5	1.4312	5
3	0	-4	2.2591	8	2.2465	7	4	2	2	1.4249	8	1.4238	7
1	2	2	2.2117	9	2.2102	8	2	4	2	1.2550	5	1.2536	5

of this ion combination corresponds to 23 electrons and is between Ca (20 electrons) and Mn (25 electrons). Consequently, the structural study (Sokolova *et al.*, 1991) strongly suggests that this mineral also has dominant Mn^{2+} on A1.

Average bond lengths for manganiandrosite-(Ce) and vanadoandrosite-(Ce) are within standard deviations very similar. However, the M1 site in manganiandrosite-(Ce) is much more distorted than the corresponding site in vanadoandrosite-(Ce). This difference is attributed to the Jahn-Teller active role of Mn^{3+} in manganiandrosite-(Ce). In the latter mineral the difference between the shortest (M1-O4) and the longest (M1-O1) distance amounts to 0.227 Å, very similar to 0.231 Å for manganiandrosite-(La) (Bonazzi *et al.*, 1996). In contrast, the corresponding difference in vanadoandrosite-(Ce) is only 0.161 without Mn^{3+} on M1. Ferriallanite-(Ce) (Kartashov *et al.*, 2002), simplified $CaCeFe^{3+}Al$-$Fe^{2+}SiO_4Si_2O_7O(OH)$, has a M1-O1, M1-O4 difference of only 0.107 Å which confirms the interpretation that large differences are caused by the Mn^{3+} Jahn-Teller effect. Interestingly, O1 and O4 define the common edge between M1

and M3 octahedra. O4 bonds twice to M1, once to M3, and also acts as acceptor of the weak hydrogen bond with O10 as donor. Simple bond-valence arguments indicate that O4 is underbonded; thus M1-O4 and M3-O4 distances are rather short even in clinozoisite $Ca_2Al_3SiO_4Si_2O_7O(OH)$ (Comodi & Zanazzi, 1997). Underbonding of O4 in androsite is further increased because M3 is occupied by Mn^{2+}. Thus, the octahedral O4-M1-O4 axis is the preferred direction of contraction for Jahn-Teller active cations (Mn^{3+}) on M1. This is also evident from a comparison of M1-O4 (1.930 Å) in ferriallanite-(Ce) (Kartashov *et al.*, 2002), M1-O4 (1.914 Å) in vanadoandrosite-(Ce) on one hand and M1-O4 (1.863 Å) for manganiandrosite-(La) (Bonazzi *et al.*, 1996) and M1-O4 (1.885 Å) for manganiandrosite-(Ce) on the other hand. One may also predict that the hydrogen bond between O4 and O10 is strengthened if M3 is occupied by M^{2+}. In fact, the donor-acceptor (O10-O4) distance in piemontite is 2.95 Å (Ferraris *et al.*, 1989), but 2.87 Å in manganiandrosite-(Ce) and vanadoandrosite-(Ce).

Discussion

Mn-rich REE-silicates and oxidation state

Manganese deposits commonly contain several transition elements, which offer a spectrum of oxygen fugacity indicators through the coexistence (or not) of some of the V^{3+}, V^{5+}, Fe^{2+}, Fe^{3+}, Mn^{2+}, Mn^{3+} and Mn^{4+} ions in crystals. The REE-bearing epidote-group minerals are able to accommodate many of these ions and are therefore an interesting gauge in this respect. The Alpine deposits with abundant hematite–braunite–piemontite quartzite represent highly oxidized systems with neither Fe^{2+} nor V^{3+} stable, but coexisting Fe^{3+}, Mn^{2+}, Mn^{3+} and, locally, V^{5+}. The latter ion obviously does not enter the epidote structure but typically occurs in the rare vanadatosilicate medaite, $Mn_6[VSi_5O_{18}(OH)]$ (in the Ligurian Apennines), or substitutes for tetrahedral As in arsenatosilicates like ardennite (common in the Western Alps deposits, *e.g.* Pasero & Reinecke, 1991; Pasero *et al.*, 1994) or like the rare tiragalloite, $Mn_4[AsSi_3O_{12}(OH)]$, which also occurs in the Haute Maurienne, Western Alps (Cenki-Tok & Chopin, 2006). On the other hand, vanadium in the Pyrenean Vielle Aure deposit occurs essentially in the trivalent state, substituting for octahedral Al in spessartine (Table 1, anal. 3) and muscovite (Ragu, 1990), in the spinel vuorelainenite (*ca.* 48 wt% V_2O_3, 22 wt% MnO, 23 wt% FeO_{total}) and in vanadoandrosite-(Ce). This lower oxidation state than in the Alpine deposit is entirely consistent with the presence of essentially divalent Mn and both Fe^{2+} and Fe^{3+} in the Pyrenean vanadoandrosite (*versus* solely Fe^{3+} and both Mn^{2+} and Mn^{3+} in the Alpine manganiandrosite), as derived by charge balance in the recalculation of the formulae given in the Mineral chemistry section. Note, however, that these valence ratios are quite sensitive to the assumption made on A-site occupancy (*cf.* Table 1, in which vacancies are taken at face value). At the same or slightly higher oxidation state but in Mn-rich and V-free systems, one can ex-
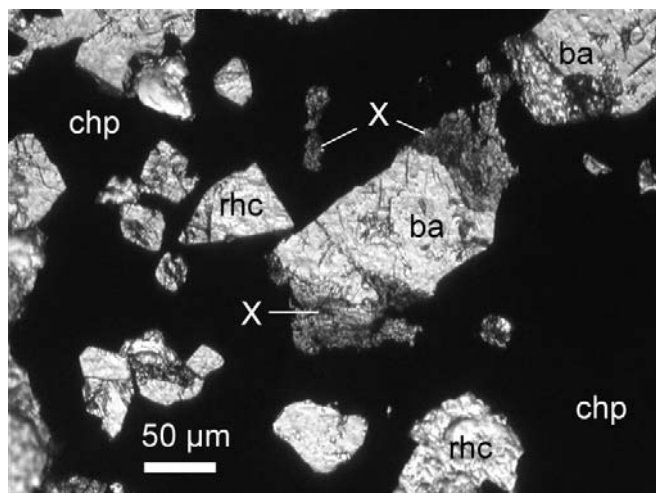
pect a potential 'ferriandrosite', $Mn^{2+}(REE)$ $Fe^{3+}AlMn^{2+}$ $SiO_4Si_2O_7O(OH)$, to become stable. A still higher oxidation state will let Mn^{3+} compete with Fe^{3+} in M1, stabilizing manganiandrosite proper. In the Praborna sample, significantly, Mn^{3+} prevails over Fe^{3+} at M1 (therefore manganiandrosite) although the Fe^{3+} content is buffered to the maximum value (for given P and T) by coexisting hematite. Such and more highly oxidized systems can produce another extremely Mn-rich REE-silicate, stavelotite-(La), ideally $La_3Mn^{2+}_3Cu^{2+}(Mn^{3+},Fe^{3+},Mn^{4+})_{26}[Si_2O_7]_6O_{30}$, albeit probably at lower metamorphic grade (Bernhardt *et al.*, 2005). The question arises whether the occurrence of the La-dominant members of manganiandrosite (Bonazzi *et al.*, 1996) and stavelotite (Bernhardt *et al.*, 2005) in such highly oxidized systems is fortuitous or reflects incipient oxidation of cerium to the tetravalent state. Our finding of manganiandrosite-(Ce) in Praborna suggests that bulk-chemical effects rather than oxidation may be more effective in this respect.

Other Mn- or V-rich REE-bearing epidote-group minerals

Samples collected at Vielle Aure and other workings of the Pyrenean Mn-district reveal a compositional variety of epidote-group minerals, which most likely reflects local bulk-rock compositional variations. In sample CP851, in a groundmass of microcrystalline quartz, rare and tiny crystals of allanite-like epidote (with friedelite and pyrite) are more Al- and Ca-rich and less V- and Mn-rich than the two vanadoandrosite samples (Table 1, anal. 5). Formula recalculation as above leads to
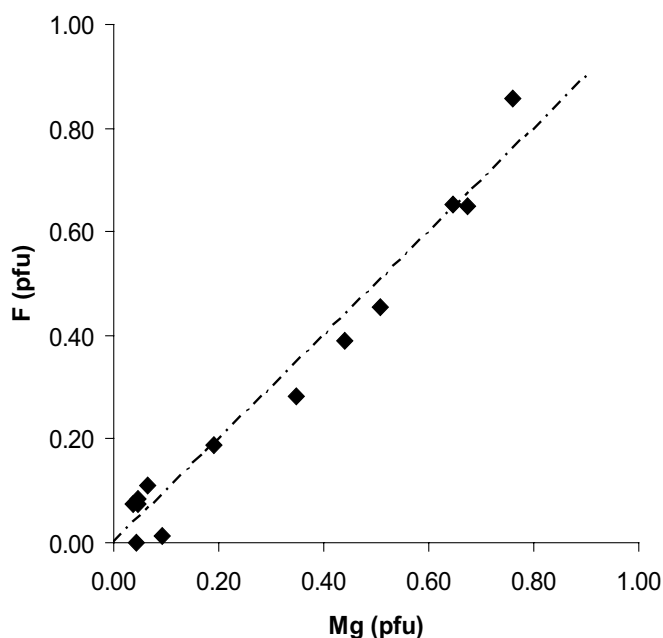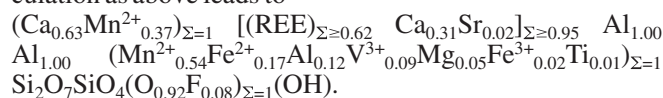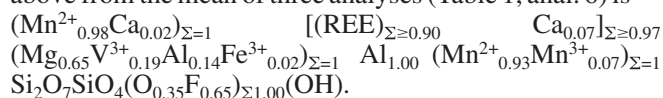
$(Ca_{0.63}Mn^{2+}_{0.37})_{\Sigma=1}$ $[(REE)_{\geq 0.62}$ $Ca_{0.31}Sr_{0.02}]_{\Sigma \geq 0.95}$ $Al_{1.00}$ $Al_{1.00}$ $(Mn^{2+}_{0.54}Fe^{2+}_{0.17}Al_{0.12}V^{3+}_{0.09}Mg_{0.05}Fe^{3+}_{0.02}Ti_{0.01})_{\Sigma=1}$ $Si_2O_7SiO_4(O_{0.92}F_{0.08})_{\Sigma=1}(OH)$.

Fig. 4. Polycrystalline overgrowth of an allanite-looking, potentially new epidote-group mineral [X, close to MnCe MgAlMn $Si_3O_{11}F(OH)$] on chalcopyrite (chp) with barite (ba) inclusions, in a rhodochrosite (rhc) groundmass. Sample VAIN86, Vielle Aure, Pyrénées; photomicrograph, plane polarized light.

Fig. 5. Magnesium *vs.* fluorine atomic contents in Mn- and REE-rich epidote-group minerals from the Pyrénées; samples CP851 and VAI series. The 1:1 line is for comparison.

Whatever site Mg and V are assigned to, the formula shows dominant Ca in A1, dominant REE in A2, dominant Al in both M1 and M2, and Mn^{2+} as the dominant charge-compensating cation in M3. This is therefore a potential new member of the allanite sub-group, with end-member formula $Ca(REE) AlAlMn^{2+} SiO_4Si_2O_7O(OH)$, *i.e.* the Mn^{2+} analogue of allanite and dissakisite. In sample VAIN86 (Fig. 4) an allanite-like mineral overgrows chalcopyrite associated with barite, in a rhodochrosite groundmass. The composition is virtually Ca- and Fe-free (!), very Mn-rich, and the high Mg-contents (up to 5 wt % MgO) are in keeping with high F contents, suggesting a dollaseite-type substitution. The structural formula recalculated as above from the mean of three analyses (Table 1, anal. 6) is $(Mn^{2+}_{0.98}Ca_{0.02})_{\Sigma=1}$ $[(REE)_{\Sigma\geq0.90}$ $Ca_{0.07}]_{\Sigma\geq0.97}$ $(Mg_{0.65}V^{3+}_{0.19}Al_{0.14}Fe^{3+}_{0.02})_{\Sigma=1}$ $Al_{1.00}$ $(Mn^{2+}_{0.93}Mn^{3+}_{0.07})_{\Sigma=1}$ $Si_2O_7SiO_4(O_{0.35}F_{0.65})_{\Sigma1.00}(OH)$.

It is close to the end-member formula $Mn^{2+}(REE)$ $MgAlMn^{2+} SiO_4Si_2O_7F(OH)$, which is actually either that of khristovite if our re-interpretation of it with dominant Mn^{2+} in A1 is correct, or a new species in case Ca is confirmed as the dominant A1 cation in khristovite. In any event, this occurrence demonstrates that the dollaseite-type substitution is as effective in the manganiandrosite series as it is in the allanite series. Figure 5 shows the range of Mg and F contents measured in our samples; their correlation is close to 1:1 which implies that, even in such profusely Mn-rich systems, Mg rather than Mn is specifically incorporated (most likely in M1) for charge-balance of F at the O4 site.

An oxidation state similar to that of the vanadoandrosite holotype sample pertains for the V-rich allanite reported by Kato *et al*. (1994) from the Odaki Mn-orebody in Japan: V^{3+} coexists with Mn^{2+}, Fe^{2+} and Fe^{3+} in this allanite (Table 1, anal. 7–8), but the system is not Mn-rich enough to allow dominant Mn in M3 and A1 (*i.e.* to form vanadoandrosite). Their phase is actually a potential 'vanadoallanite' with the end-member formula $Ca(REE) V^{3+}AlFe^{2+} SiO_4Si_2O_7O(OH)$, assuming V partitioning into M1 as shown in the present work.

Practical implications

The site assignments derived from the structure refinements of the two Mn- and REE-rich epidote-group minerals studied here establish two main points.

– They confirm that divalent Mn is indeed a major occupant of the large A1 site, as shown by Bonazzi *et al*. (1992, 1996). It may even be preferentially partitioned into this site over the large M3 octahedral site, in case other divalent cations are present in the system and can occupy M3, *e.g.* if oxidation state allows divalent iron (*cf*. #VAI586). [This is most likely also the case in the two Mn-rich 'allanites' (from pegmatite) analysed by Hasegawa (no. 9 and 10 in Table 1, from Deer *et al*., 1997; *cf*. Hoshino *et al*., 2006), for which the formula recalculation shows dominant Mn^{2+} in A1 and dominant Fe^{2+} in M3]. A practical implication is that the empirical formula of Mn-bearing epidote-group minerals should *not* be calculated on the basis of a fixed number of tetrahedral + octahedral cations (the "superior" method no.

10 of Ercit, 2002), because Mn commonly occupies another, larger site.

– V^{3+} is strongly partitioned into the M1 site while the charge compensation for REE takes place in M3. A tempting consequence is then the making of a 'vanadoallanite' from Kato *et al*.'s (1994) vanadian 'allanite' (see above), following the same line as for the naming of ferriallanite (Kartaschov *et al*., 2002). It is unlikely that this partitioning pattern can be extended to the *REE-free* mukhinite (Shepel & Karpenko, 1969), for which one rather expects Al in M1 (and M2) and V^{3+} in M3 on the basis of ionic size, but this awaits structural confirmation. As to the V-rich (up to *ca*. 9 wt % V_2O_3), Mn-poor 'allanites' analysed by Pan & Fleet (1991), the Al-contents are also high enough to fill M2 and most of the M1 site for all crystals that have REE dominant in A2, so that the presence of V in M3, even in substantial amount, should logically be subordinated to the divalent, charge-compensating cations in this site and so does not warrant a new name (see below).

A further point is the good agreement between the site populations derived from the crystallographic study and those obtained from the chemical data by site assignment on the basis of increasing ionic radius (from M2 to M3 through M1). The result is encouraging and shows that, in the absence of structure refinement, this ionic-size basis can serve as a relatively safe assumption for site allocation when recasting empirical chemical formulae of epidote-group minerals into structural formulae.

In summary, on the basis of the present description and literature data, the following new members can be found among Mn- or V-rich REE-bearing epidotes, with end-member formulae:
$Mn^{2+}REE V^{3+}AlMn^{2+} SiO_4Si_2O_7O(OH)$, vanadoandrosite,
$Mn^{2+}REE MgAlMn^{2+} SiO_4Si_2O_7F(OH)$, sample VAIN86,
$Mn^{2+}REE AlAlFe^{2+} SiO_4Si_2O_7O(OH)$, Hasegawa in Deer *et al*. (1997),
$CaREE AlAlMn^{2+} SiO_4Si_2O_7O(OH)$, sample CP851,
$CaREE V^{3+}AlFe^{2+} SiO_4Si_2O_7O(OH)$, Kato *et al*. (1994).

The rule of the 'site-dominant cation'

Finally, it may be worth emphasizing one of the nomenclature criteria chosen for these two new minerals, namely that the root-name androsite applies if Mn^{2+} is the *dominant charge-compensating* cation in M3. This acknowledges the central crystal-chemical role of the coupled heterovalent substitutions of Ca by REE in A2 and of Al by Me^{2+} in M3: if REE are dominant in A2, significant is that Me^{2+} cations are dominant in M3 for charge balance, regardless of the fact that a trivalent cation may be more abundant at this site than any of the charge-compensating cations taken individually, in case of multiple occupancy. This is why the dominant charge-compensating cation is considered for nomenclature, rather than the site-dominant cation. This rephrasing of the dominant-cation rule is of general bearing, as exemplified in the arrojadite-dickinsonite group (Chopin *et al*., 2006) and as explicitly dealt with in the new nomenclature of the whole epidote group (Armbruster *et al*., 2006).

References

Armbruster, T., Bonazzi, P., Akasaka, M., Bermanec V., Chopin, C., Gieré, R., Heuss-Assbichler, S., Liebscher, A., Menchetti, S., Pan, Y., Pasero, M. (2006): Recommended nomenclature of epidote-group minerals. *Eur. J. Mineral.*, **18**, 551–567.

Bermanec, V., Armbruster, T., Oberhänsli, R., Zebec, V. (1994): Crystal chemistry of Pb- and REE-rich piemontite from Nezilovo, Macedonia. *Schweiz. mineral. petrogr. Mitt.*, **74**, 321–328.

Bernhardt, H.-J., Armbruster, T., Fransolet, A.-M., Schreyer, W. (2005): Stavelotite-(La), a new lanthanum-manganese-sorosilicate mineral from the Stavelot Massif, Belgium. *Eur. J. Mineral.*, **17**, 703–714.

Bonazzi, P. & Menchetti, S. (1995): Monoclinic members of the epidote group: effects of the Al $\leftrightarrow$ Fe^{3+} $\leftrightarrow$ Fe^{2+} substitution and of the entry of REE^{3+}. *Mineral. Petrol.*, **53**, 133–153.

—, — (2004): Manganese in monoclinic members of the epidote group: Piemontite and related minerals. In: Epidotes. *Reviews in Mineralogy & Geochemistry*, **56**, 495–552.

Bonazzi, P., Menchetti, S., Palenzona, A. (1990): Strontiopiemontite, a new member of the epidote group from Val Graveglia, Liguria, Italy. *Eur. J. Mineral.*, **2**, 519–523.

Bonazzi, P., Garbarino, C., Menchetti, S. (1992): Crystal chemistry of piemontites: REE-bearing piemontite from Monte Brugiana, Alpi Apuane, Italy. *Eur. J. Mineral.*, **4**, 23–33.

Bonazzi, P., Menchetti, S., Reinecke, T. (1996): Solid solution between piemontite and androsite-(La), a new mineral of the epidote group from Andros island, Greece. *Am. Mineral.*, **81**, 735–743.

Brugger, J., Gieré, R., Graeser, S., Meisser, N. (1997): The crystal chemistry of roméite. *Contrib. Mineral. Petrol.*, **127**, 136–146.

Brugger, J., Bonin, M., Schenk, K.J., Meisser, N., Berlepsch, P., Ragu, A. (1999): Description and crystal structure of nabiasite, BaMn$_9$[(V,As)O$_4$]$_6$(OH)$_2$, a new mineral from Central Pyrénées (France). *Eur. J. Mineral.*, **11**, 879–890.

Carbonin, S. & Molin, G. (1980): Crystal chemical considerations on eight metamorphic epidotes. *N. Jb. Mineral. Mh.*, **1980**, 205–215.

Catti, M., Ferraris, G., Ivaldi, G. (1988): Thermal behavior of the crystal structure of strontian piemontite. *Am. Mineral.*, **73**, 1370–1376.

—, —, — (1989): On the crystal chemistry of strontian piemontite with some remarks on the nomenclature of the epidote group. *N. Jb. Mineral. Mh.*, **1989**, 357–366.

Cenki-Tok, B. & Chopin, C. (2006): Coexisting calderite and spessartine garnets in eclogite-facies metacherts of the Western Alps. *Mineral. Petrol.*, in press.

Chopin, C. (1978): Les paragenèses réduites ou oxydées de concentrations manganésifères des "schistes lustrés" de Haute-Maurienne (Alpes françaises). *Bull. Minéral.*, **101**, 514–531.

— (1981a): Talc-phengite: a widespread assemblage in high-grade pelitic blueschists of the Western Alps. *J. Petrol.*, **22**, 628–650.

— (1981b): Mise en évidence d'une discontinuité du métamorphisme alpin entre le massif du Grand Paradis et sa couverture allochtone (Alpes occidentales françaises). *Bull. Soc. géol. France* (7), **23**, 297–301.

Chopin, C., Oberti, R., Cámara, F. (2006): The arrojadite enigma: II. Compositional space, new members and nomenclature of the group. *Am. Mineral.*, **91**, in press.

Comodi, P. & Zanazzi, P.F. (1997): The pressure behavior of clinozoisite and zoisite: An X-ray diffraction study. *Am. Mineral.*, **82**, 61–68.

Cortesogno, L., Luchetti, G., Penco, A.M. (1979): Le mineralizzazioni a manganese nei diaspri delle ofioliti liguri : mineralogia e genesi. *Rend. Soc. Ital. Mineral. Petrol.*, **35**, 151–197.

Dal Piaz, G.V., Di Battistini, G., Kienast, J.-R., Venturelli, G. (1979): Manganiferous quartzitic schists of the Piemonte ophiolitic nappe. *Mem. Sci. Geol. Padova*, **32**, 1–24.

Dal Piaz, G.V., Cortiana, G., Del Moro, A., Martin, S., Pennacchioni, G., Tartarotti, P. (2001): Tertiary age and paleostructural inferences of the eclogitic imprint in the Austroalpine outliers and Zermatt-Saas ophiolite, western Alps. *Int. J. Earth Sci.*, **90**, 668–684.

Damour, A. (1841): Sur la roméite, nouvelle espèce minérale, de St Marcel, Piémont. *Annales des Mines*, 3rd ser. **20**, 247.

Deer W.A., Howie, R.A., Zussman, J. (1997): Rock forming minerals. Vol. 1B, Disilicates and ring silicates. 2nd edition. The Geological Society London, 630 p.

Ercit, T.S. (2002): The mess that is allanite. *Can. Mineral.*, **40**, 1411–1419.

Ferraris, G., Ivaldi, G., Fuess, H., Gregson, D. (1989): Manganese/iron distribution in a strontian piemontite by neutron diffraction. *Z. Kristallogr.*, **187**, 145–151.

Gabe, E.J., Portheine, J.C., Whitlow, S.H. (1973): A reinvestigation of the epidote structure: Confirmation of the iron location. *Am. Mineral.*, **58**, 218–223.

Gibbs, G.V. (1982): Molecules as models for bonding in silicates. *Am. Mineral.*, **67**, 421–450.

Grew, E.S., Essene, E.J., Peacor, D.R., Su, S.C., Asami, M. (1991): Dissakisite-(Ce), a new member of the epidote group and the Mg analog of allanite-(Ce), from Antarctica. *Am. Mineral.*, **76**, 1990–1997.

Gruppo Ofioliti (1977): Escursione ad alcuni giacimenti a Cu-Fe e Mn della falda piemontese, Alpi occidentali : 10–13 ottobre 1977. *Ofioliti*, **2**, 241–263.

Hoshino, M., Kimata, M., Shimizu, M., Nishida N., Fujiwara, T. (2006): Allanite-(Ce) in granitic rocks from Japan: genetic implications of patterns of REE and Mn enrichment. *Can. Mineral.*, **44**, 45–62.

Kartashov, P.M., Ferraris, G., Ivaldi, G., Sokolova E., McCammon C.A. (2002): Ferriallanite-(Ce), CaCeFe^{3+}AlFe^{2+}(SiO$_4$)(Si$_2$O$_7$)O(OH), a new member of the epidote group: description, X-ray and Mössbauer study. *Can. Mineral.*, **40**, 1641–1648.

Kato, A., Shimizu, M., Okada, Y., Komuro, Y., Takeda, K. (1994): Vanadium-bearing spessartine and allanite in the manganese-iron ore from the Odaki orebody of the Kyurazawa Mine, Ashio Town, Tochigi Prefecture, Japan. *Bull. Nat. Mus. Tokyo, ser. C*, **20**, 1–12.

Kenngott, A. (1853): *Das Mohs'sche Mineralsystem.* (Piemontit). p. 75.

Lacroix, A. (1900): Sur les minéraux des gisements manganésifères des Hautes Pyrénées. *Bull. Soc. fr. Minéral.*, **23**, 251–253.

Mandarino, J.A. (1976): The Gladstone-Dale relationship – Part 1. Derivation of new constants. *Can. Mineral.*, **14**, 498–502.

Marchesini, M. & Pagano, R. (2001): The Val Graveglia manganese district, Liguria, Italy. *Mineral. Record*, **32**, 349–379.

Martin, S. & Kiénast, J.R. (1987): The HP-LT manganiferous quartzites of Praborna, Piemonte ophiolite nappe, Italian Western Alps. *Schweiz. mineral. petrogr. Mitt.*, **67**, 339–360.

Martin, S. & Polino, R. (1984): Le metaradiolariti a ferro di Cesana (Valle di Susa – Alpi Occidentali). *Mem. Soc. Geol. It.*, **29**, 107–125.

Martin, S. & Tartarotti, P. (1989): Polyphase HP metamorphism in the ophiolitic glaucophanites of the lower St. Marcel valley (Aosta, Italy). *Ofioliti*, **14**, 135–156.

Medenbach, O. (1986): Ein modifiziertes Kristallbohrgerät nach Verschure (1978) zur Isolierung kleiner Einkristalle aus Dünnschliffen. *Fortschr. Mineral.*, Beiheft 1, **64**, 113.

Meisser, N., Perseil, E.A., Brugger, J., Chiappero, P.J. (1999): Strontiomelane, $SrMn^{4+}_6Mn^{3+}_2O_{16}$, a new mineral species of the cryptomelane group from St. Marcel-Praborna, Aosta Valley, Italy. *Can. Mineral.*, **37**, 673–678.

Mottana, A., Rossi, G., Kracher, A., Kurat, G. (1979): Violan revisited: Mn-bearing omphacite and diopside. *Tschermaks Min. Petr. Mitt.*, **26**, 187–201.

Pan, Y. & Fleet, M.E. (1991): Vanadian allanite-(La) and vanadian allanite-(Ce) from the Hemlo gold deposit, Ontario, Canada. *Mineral. Mag.*, **55**, 497–507.

Pasero, M. & Reinecke, T. (1991): Crystal chemistry, HRTEM analysis and polytypic behaviour of ardennite. *Eur. J. Mineral.*, **3**, 819–830.

Pasero, M., Reinecke, T., Fransolet, A.-M. (1994): Crystal structure refinements and compositional control of Mn–Mg–Ca ardennites from the Belgian Ardennes, Greece, and the Western Alps. *N. Jb. Mineral. Abh.*, **166**, 137–167.

Pautov, L.A., Khvorov, P.V., Ignatenko, K.I., Sokolova, E.V., Nadezhina, T.N. (1993): Khristovite-(Ce), (Ca,REE)REE(Mg,Fe)MnAlSi$_3$O$_{11}$(OH)(F,O). *Proceed. Russian Mineral. Soc.*, **122**, 103–111 (in Russian).

Peacor, D.R. & Dunn, P.J. (1988): Dollaseite-(Ce) (magnesium orthite redefined). Structure refinement and implications for F^- + M^{2+} substitutions in epidote-group minerals. *Am. Mineral.*, **73**, 838–842.

Ragu, A. (1990): Pétrologie et minéralogie des minéralizations manganésées métamorphiques dans le Paléozoïque des Pyrénées Centrales. *Mémoire des Sciences de la Terre*, no. 90-**15** (Univ. P. et M. Curie, Paris, ed.), 328 p.

— (1994): Helvite from the French Pyrénées as evidence for granite related hydrothermal activity. *Can. Mineral.*, **32**, 111–120.

Reinecke, T. (1991): Very-high-pressure metamorphism and uplift of coesite-bearing metasediments from the Zermatt-Saas zone, Western Alps. *Eur. J. Mineral.*, **3**, 7–17.

Rouse, R.C. & Peacor, D.R. (1993): The crystal structure of dissakisite-(Ce), the Mg-analogue of allanite-(Ce). *Can. Mineral.*, **31**, 153–157.

Sheldrick, G.M. (1997): SHELXL-97 Program for refinement of crystal structures. University of Göttingen, Germany.

Shepel, A.V. & Karpenko, M.V. (1969): Mukhinite, a new vanadium species of epidote. *Dokl. Acad. Nauk SSSR*, **185**, 1342–1345 (in Russian).

Sokolova, E.V., Nadezhina, T.N., Pautov, L.A. (1991): Crystal structure of a new natural silicate of manganese from the epidote group. *Sov. Phys. Crystallogr.*, **36**, 172–174.

Stergiou, A.C., Rentzeperis, P.J., Sklavounos, S. (1987): Refinement of the crystal structure of a medium iron epidote. *Z. Kristallogr.*, **178**, 297–305.

Tumiati, S. (2005): Geochemistry, mineralogy and petrology of the eclogitized manganese deposit of Praborna (Val d'Aosta, Italian Western Alps). PhD thesis, Université Paris 7 / Università dell'Insubria, 241 p.

Yvon, K., Jeitschko, W., Parthé, E. (1977): LAZY-PULVERIX, a computer program, for calculating X-ray and neutron diffraction powder patterns. *J. Appl. Crystallogr.*, **10**, 73–74.